Int J Appl Earth Obs Geoinformation 68 (2018) 31–41

Contents lists available at ScienceDirect

Int J Appl Earth Obs Geoinformation

journal homepage: www.elsevier.com/locate/jag

Multi-platform assessment of turbidity plumes during dredging operations in a major estuarine system

Isabel Caballero*, Gabriel Navarro, Javier Ruiz

Institute of Marine Sciences of Andalusia (ICMAN), National Research Council (CSIC), Department of Ecology and Coastal Management, 11519 Puerto Real, Cádiz, Spain

ARTICLE INFO

Keywords:
Medium and high-resolution satellites
Atmospheric correction
Dredging activities
Total suspended solids
Guadalquivir estuary

ABSTRACT

Dredging activities in estuaries frequently cause deleterious environmental effects on the water quality which can impact flora, fauna, and hydrodynamics, among others. A medium- and high-resolution satellite-based procedure is used in this study to monitor turbidity plumes generated during the dredging operations in the Guadalquivir estuary, a major estuarine system providing important ecosystem services in southwest Europe. A multi-sensor scheme is evaluated using a combination of five public and commercial medium- and high-resolution satellites, including Landsat-8, Sentinel-2A, WorldView-2, WorldView-3, and GeoEye-1, with pixel sizes ranging from 30 m to 0.3 m. Applying a multi-conditional algorithm after the atmospheric correction of the optical imagery with ACOLITE, Sen2Cor and QUAC processors, it is demonstrated the feasibility to monitoring suspended solids during dredging operations at a spatial resolution unachievable with traditional satellite-based ocean color sensors (> 300 m). The frame work can be used to map on-going, post and pre-dredging activities and asses Total Suspended Solids (TSS) anomalies caused by natural and anthropogenic processes in coastal and inland waters. These promising results are suitable to effectively improve the assessment of features relevant to environmental policies for the challenging coastal management and might serve as a notable contribution to the Earth Observation Program.

1. Introduction

Dredging activities are a frequent requirement for the creation of new and the maintenance of existing coastal infrastructures, including navigable waterways, harbors, and river channels, which have an important role in the economic and commercial growth of many nations. Dredging projects, both major works and recurring maintenance operations, are often approved under regulations based on an assessment of their environmental impact (CEDA, 2011, 2015) as they may modify water quality conditions by increasing the concentration of suspended matter and contamination (Johnston, 1981). The presence of pollutants in coastal waters after dredged material is disposed has created concern for its expected impact on both wildlife and humans (Newell et al., 1998; CEDA, 2011), leading to the mandatory requirement of sediment and turbidity mapping during operations to ensure acceptable water quality levels are maintained according to baseline conditions prior to dredging (CEDA, 2015).

Traditionally, in-situ sampling and laboratory analysis are used for this monitoring to detect the spatio-temporal extent of the turbidity plume, as well as continuous telemetered loggers for turbidity. These methodologies provide high temporal density data, which when combined with concepts around sentinel sites have been very effective for dredging operation management (CEDA, 2011, 2015). Nevertheless, these approaches are substantially time-consuming and expensive as well as limited in the spatial resolution they offer. Within this context, effective and cost-efficient Remote Sensing (RS) technologies may provide significant improvements on conventional monitoring methodologies. Currently, RS is at the crossroads in terms of ocean and coastal management to guide socio-economic decisions, while governments and industry are focusing upon adapting to a changing environment (IOCCG, 2012). Although application of remote optical sensors on water quality studies is recognized in the science community as a high priority activity (IOCCG, 2012), fine scale monitoring of suspended material during dredging operations has not been regularly implemented despite its potential for improving on commonly adopted methods. Previous works highlighted the capacities of RS imagery to estimate the environmental effects during dredging activities (Jørgensen and Edelvang, 2000; Sipelgas et al., 2006; Islam et al., 2007; Evans et al., 2012; Barnes et al., 2015; Vanhellemont and Ruddick, 2015; Fearns et al., 2017; Seo et al., 2018). Evans et al. (2012) developed a RS approach to monitor the daily extent of dredge plumes using Moderate Resolution Imaging Spectroradiometer (MODIS) imagery in a

* Corresponding author. Present address: NOAA National Centers for Coastal Ocean Science, 1305 East West Highway, Silver Spring, MD, 20910, USA.
E-mail address: Isabel.caballero@icman.csic.es (I. Caballero).

https://doi.org/10.1016/j.jag.2018.01.014
Received 23 August 2017; Received in revised form 22 January 2018; Accepted 27 January 2018

case study at Barrow Island, Western Australia, with accurate results at determining plume boundaries over shallow benthic features. Simultaneous satellite and ship-borne surveys have been conducted by Seo et al. (2018) to evaluate the dispersion patterns of dredging plumes off the south coast of Korea. Dorji and Fearns (2017) investigated the impact of different spatial resolutions of satellite sensors on the quantification of Total Suspended Solid (TSS) concentration in coastal waters of northern Western Australia, demonstrating that degrading the spatial resolution led to highly variable concentrations. The great potential of RS data to operationally supplement existing data in rivers with two-dimensional information on near-surface turbidity distributions at larger spatial scales than in-situ measurements has been described by Hucke et al. (2016). A recent review of RS of dredging operations suggested this method can provide a broad overview of the dredge affected areas and is the only available technology that offers complete daily coverage over coastal waters (Fearns et al., 2017). However, there is a general consensus that more effort is required to generate innovative tools to integrate both public and commercial imagery into dredging projects and to propose new information over the decision-making area for operations, especially during large scale and multi-year projects (including maintenance works).

The new generation of medium-resolution multispectral sensors on board the Sentinel-2 twin mission (10 m) in the framework of the Copernicus Programme and Landsat-8 satellite (30 m) has increased the range of applications for coastal and inland water monitoring (Malenovský et al., 2012; Pahlevan et al., 2017). In addition, since the recent accessibility to the very high-resolution products associated with the WorldView-1/-2/-3 and GeoEye-1 missions (up to 0.30 m) supported by ESA within the Third Party Missions (TPM) initiative for research and application development, new perspectives of Earth Observing System data products by RS can be achieved. Specifically, these emerging technologies will provide a unique set of accurate and timely information improving the management of the marine environment, particularly with the assistance to support European operational and policy needs for water quality monitoring.

This study aims to use a combination of this emerging optical data to assist for the challenging monitoring of TSS during dredging operations and assess the potential impacts of dredging activities on water quality. The objective is to meet the growing demand for high-resolution satellite imagery able to provide relevant and cost-efficient information for dredging design and operation in coherence with increasing monitoring requirements imposed by environmental policies and regulations. The approach is focused on the last of a series of dredging projects conducted from October to December 2016 in the Guadalquivir estuary (Fig. 1), the largest estuary in southwest Europe. This is an excellent opportunity to investigate the dredging-induced plume of suspended solids using medium and high-resolution optical imagery from different platforms, both public (Landsat-8 and Sentinel-2A) and commercial (WorldView-2/3 and GeoEye-1), in a combination of processing techniques able to monitor the impact of dredging operations at unprecedented fine-scale resolution. The purpose is to extend, but not to substitute, the existing in-situ measurements from the near surface part of the water column. We focus on the Atmospheric Correction (AC) of the imagery data using different procedures, the inspection of the TSS products, and we then go on to demonstrate the potential of this multi-platform imagery scheme for the retrieval of detailed information about TSS dynamics within the estuary channel.

2. Study area, data sets and methods

2.1. The Guadalquivir estuary

The Guadalquivir River is located in the southwest of the Iberian Peninsula (Fig. 1) and corresponds to one of the largest rivers in Spain (650 km long). Its estuary has a width of 800 m near the mouth to 150 m at the head and is a provider of key ecosystem services in the region (Ruiz et al., 2015). Tidal influence extends up the Guadalquivir as far as the Alcalá del Río dam (Díez-Minguito et al., 2012), 110 km upstream from the river mouth at Sanlúcar de Barrameda (Fig. 1c). The estuary is a well mixed mesotidal system with a longitudinal salinity gradient (Vanney, 1970), a semidiurnal tidal period and maximum tidal range of 3.86 m. Up to now, operational river monitoring and sediment management in the estuary mainly rely on in-situ measurements and on results obtained from numerical modelling (Navarro et al., 2011, 2012; Díez-Minguito et al., 2012, 2014; Ruiz et al., 2015, 2017). These studies confirmed strong mixing is typical along the estuary, with surface samples representative of values in most of the water column (Díez-Minguito et al., 2012, 2014; Flecha et al., 2015). During the last decades, the adjacent region has undergone substantial changes in agricultural land use, urban development, and fisheries extraction (Ruiz et al., 2015; Vargas and Paneque, 2015). As a consequence, the current shape of the estuary is characterized by a main channel surrounded by tidal creeks without any significant intertidal zones.

The relatively heavy commercial and tourist traffic requires the periodic dredging of the estuary shipping channel. This routine dredging is carried out every year from its mouth to where it accesses the Port of Seville in order to guarantee a minimum navigation depth of 6.5 m (Vargas and Paneque, 2015; Donázar-Aramendía et al., 2016). Rise crops, aquaculture, fishing, industry and the touristic sector are major activities carried out in this area which strongly depend on maintaining good water quality conditions under dredging periods (Vargas and Paneque, 2015). Dredging also has the potential to impact the Natural and National Park of Doñana located at the mouth of the estuary (Fig. 1c), an area declared a World Heritage Site by Unesco in 1994, which is considered one of the most important conservation sites in the world (UNESCO-MAB Biosphere Reserve). It is, therefore, a hot spot where to test the methodology developed in connection with these operations. The requirement is to capture and quantitatively assess events of extreme turbidity using satellite imagery, both natural and human-induced, which are still controversial in the Guadalquivir estuary (Ruiz et al., 2015, 2017; Vargas and Paneque, 2015), focusing on the last of a series of dredging projects conducted from October to December 2016..

2.2. Satellite imagery

A multi-sensor approach using several optical satellites to effectively increase revisit frequency and complement temporal gaps, a common feature of high-resolution satellite imagery, is developed. Considering the prevalence of ocean color products and characteristics, satellite data was selected from five on-orbit sensors: Landsat-8, Sentinel-2A, Worldview-2, Worldview-3, and GeoEye-1. The potential of these satellites encompasses a wide range of applications with a combination of capabilities to fulfill the satellite data requirements for fine scale ocean mapping, specifically over coastal and inland environments. The multi-sensor methodology was designed to improve the application of remotely sensed data for coastline studies through enhanced spatial, temporal, and spectral capabilities, allowing the detection of human impacts invisible at traditional ocean color resolution (0.25–1 km). Severe cloud coverage was encountered at this latitude, limiting the number of usable images. However, 6 cloud-free scenes acquired during the dredging period were utilized in analyses. The characteristics of the five sensors and images used are listed in Table 1.

Optical sensors are designed to retrieve the spectral distribution of upwelling radiance just above the sea surface (the water-leaving radiance or surface reflectance), which is then used to estimate a number of geophysical parameters (IOCCG, 2010). In this regard, AC of satellite optical data over coastal and inland waters requires effective removal of the atmospheric contribution, mainly due to absorption by gasses and aerosols and the scattering by air molecules and aerosols, from the total signal measured at Top Of Atmosphere (TOA) (IOCCG, 2010). The images were processed to Level-2 data (surface reflectance) by using

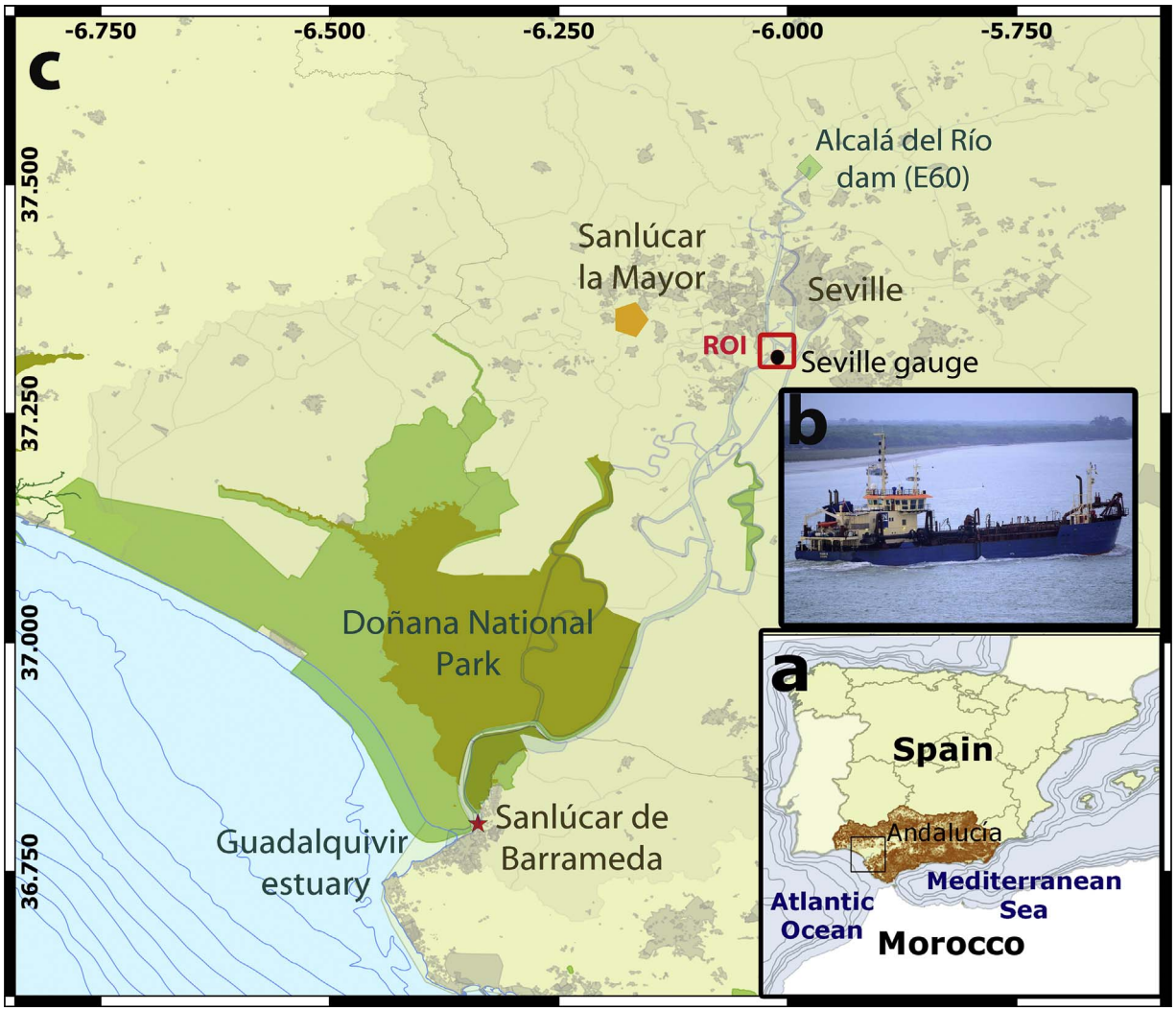

Fig. 1. a) Location of the study area (South West Iberian Peninsula); b) THOR R hopper dredger in Sanlúcar de Barrameda going up the Guadalquivir River to Seville; c) Map showing the Guadalquivir estuary environment. Red rectangle delimits the Region Of Interest (ROI). The different in-situ datasets are indicated: the Alcalá del Río dam (green diamond), the meteorological station at Sanlúcar la Mayor (orange spot), and the tidal gauge at the Port of Seville (black dot). (For interpretation of the references to colour in this figure legend, the reader is referred to the web version of this article.)

Table 1
List of the medium- and high-resolution satellites used in this study, characteristics of each satellite/image and oceano-meteorological conditions. The spatial resolution is referred to the visible and NIR bands for all the sensors, while commercial satellites also include the spatial resolution of the panchromatic bands. Area 1 (37.316°N–6.01°W) and Area 2 (37.31°N–6.019°W) correspond to two specific regions of interest along the estuary with a section of 30 × 30 m (900 m^2) with Landsat-8 as reference (see location in Fig. 3b). For the remaining satellites, arithmetic mean within the 30 × 30 m area was calculated in each case according to the different spatial resolutions. Reflectance is dimensionless (dll).

Satellite Sensor	Wave length (nm)	Spatial resolution (m)	Image Acquisition (GMT)	Atmospheric Correction	Reflectance NIR (dll) Area 1/Area 2	Hydrodynamic regime / River discharge (m^3/s) / Tidal stage (m) / Flow direction
Landsat-8 OLI	443, 483, 561, 665, 865	15–30	23 Dec.16 11:02:47	ACOLITE	0.0335/0.0405	Tidally-dominated/29/0.81/upstream
Sentinel-2A MSI	443(B1), 490(B2), 560(B3), 665(B4), 705(B5), 740(B6), 783(B7), 842(B8), 865(B8A)	10–20–60	4 Oct. 16 11:09:12	Sen2Cor/SNAP	0.0219/0.0251	Tidally-dominated/25/−0.17/ downstream
			23 Nov. 16 11:14:02		0.0289/0.0399	Intermediate/65/1.44/upstream
Wordlview-3	425, 480, 545, 605, 660, 725, 833	1.2 (0.31)	11 Nov.16 11:26:00	QUAC/ENVI	0.0353/0.0401	Tidally-dominated/16/0.15/upstream
Wordlview-2	425, 480, 545, 605, 660, 725, 833	2 (0.46)	12 Nov. 16 11:13:08	QUAC/ENVI	0.0366/0.0386	Tidally-dominated/17/0.1/upstream
GeoEye-1	480, 545, 673, 850	1.6 (0.46)	24 Nov. 16 11:16:50	QUAC/ENVI	0.0301/0.0338	Intermediate/92/0.94/upstream

three different AC procedures available in the remote sensing user community.

2.2.1. Landsat-8

The Operational Land Imager (OLI) on Landsat-8 was launched on February 2013 and is a 9 band push broom scanner with 8 channels at 30 m spatial resolution and one panchromatic channel at 15 m spatial resolution (Table 1) (Knight and Kvaran, 2014). Landsat-8 follows the Worldwide Reference System 2 orbit and has a track repeat cycle of 16 days with an equatorial crossing time at 10:00 a.m. Orthorectified and terrain corrected Level 1T OLI imagery were downloaded free of charge from EarthExplorer (http://earthexplorer.usgs.gov/) in GeoTIFF format with UTM projection datum. In this study, no images were obtained during the active dredging works since high cloud coverage limited the region of interest. However, one image immediately after dredging operations ceases was used in order to assess Landsat-8 suitability to detect TSS concentration. The image corresponds to path/row 202/34 on 23 December 2016 (Table 1).

The AC tool used was based on the recent update of the robust ACOLITE (V20170113.0) processor developed by the Royal Belgian Institute of Natural Sciences (RBINS) supporting free processing of both Landsat-8 and Sentinel-2 specifically for aquatic applications (Ruddick et al., 2016; Vanhellemont and Ruddick, 2016). In general, ACOLITE performs an AC in two steps: 1) a Rayleigh correction for scattering by air molecules, using a Look-Up Table generated using Second Simulation of the Satellite Signal in the Solar Spectrum (6SV) which considers sensor and sun geometry as well as sun and sky glint (modeled for a wind speed of 1 m/s) (Vanhellemont and Ruddick, 2015), and 2) an aerosol correction based on the assumption of black SWIR bands over water caused by the extremely high pure-water absorption, and an exponential spectrum for multiple scattering aerosol reflectance. ACOLITE outputs were expressed as dimensionless water-leaving radiance reflectance or water reflectance (hereinafter referred as ρ) in all visible and NIR bands (Vanhellemont and Ruddick, 2014, 2015). The SWIR AC option was selected with the estimation of the aerosol type using the two SWIR bands in all water pixels, allowing them to vary spatially with a moving average filter (Vanhellemont and Ruddick, 2015, 2016).

2.2.2. Sentinel-2

The Sentinel-2 optical imaging mission, in the framework of the Copernicus programme, is devoted to the operational monitoring of land and coastal areas, providing continuity to services relying on multi-spectral high-resolution optical observations over global surfaces. The constellation currently has both twin satellites Sentinel-2A and Sentinel-2B in orbit and operational. The MultiSpectral Imager (MSI) features 13 spectral bands, ranging from visible and NIR to the short wave infrared (SWIR) domains, at different spatial resolutions on the ground ranging from 10 to 60 m (Malenovský et al., 2012). Sentinel-2A images were downloaded from the Sentinel's Scientific Data Hub (https://scihub.copernicus.eu/). Data from the Sentinel-2 constellation are available openly and freely for all users. These images correspond to Level-1C (L1C) products processed by the Payload Data Ground Segment (PDGS), which means data are radiometrically and geometrically corrected TOA products (European Space Agency, 2015). The corrections include orthorectification and spatial registration on a global reference system (combined UTM projection and WGS84 ellipsoid) with sub-pixel accuracy. In this study, two images from WGS84 UTM zone 137 (STG) were considered in detail (Table 1).

Even though ACOLITE processor can also be applied to Sentinel-2 images (Vanhellemont and Ruddick, 2016), the tile containing the Port of Seville (zone 137 STG) corresponds entirely to land with no coastal waters (only the estuary channel). Therefore, the AC could not been accomplished with ACOLITE since it is designed for a minimum water coverage. Therefore, the alternative to correct Sentinel-2 data at the time of writing this study was the Sentinel-2 Toolbox (Sentinel Application Platform, SNAP v2.0.2.), which consists of a rich set of visualization, analysis and processing tools for the exploitation of MSI data from the upcoming Sentinel missions. Specifically, the AC was executed with the installation of Sen2Cor plug-in (Sentinel to Correction, v2.2.1) by (Müller-Wilm, 2016) which is a prototype processor for Sentinel-2 L2A product processing. Sen2cor performs a pre-processing of L1C TOA image data, and applies a scene classification an atmospheric, terrain and cirrus correction and a subsequent conversion into an ortho-image L2A Bottom-Of-Atmosphere (BOA, dimensionless) reflectance product (Richter et al., 2011; Müller-Wilm, 2016). Sen2Cor is configured to process with default settings including correction for adjacency effects. L2A products generated are re-sampled as L1C products with a constant Ground Sampling Distance of 10 m, 20 m and 60 m according to the native resolution of the different spectral bands (Table 1). This procedure in the common platform for the Sentinel Toolboxes will be first AC scheme accessible to the entire scientific community as open source software ideal for Earth Observation processing and analysis. Specifically, recent qualitative comparison of Sen2Cor with both ACOLITE and POLYMER procedures exhibited good performance in the Guadalquivir estuarine region (Caballero and Navarro, 2016a; Navarro and Caballero, 2017), highlighting the capacity to accomplish precise AC even if it was initially designed for land applications.

2.2.3. Commercial satellites: WorldView-2, WorldView-3, GeoEye-1

The WorldView-2/-3 and GeoEye-1 Earth Observation satellites are owned by DigitalGlobe (https://www.digitalglobe.com/) and have spectral bands in the visible to near-infrared (NIR) region with less than 2 m spatial resolution (Table 1). These archives are now available to ESA for research and application development within the framework of Third Party Missions (TPM). The images used in this study correspond to a TPM proposal (id35116) (Table 1). Specifically, the very-high-resolution of these products (up to 0.30 m in panchromatic) in addition to the spectral resolution (4–8 bands) will allow us to study the estuarine region providing a unique set of accurate, timely and easily accessible information. Imagery was acquired directly from the DigitalGlobe archive by submitting a new collection request. Standard Imagery is ordered by area, with a minimum purchase of 25 km^2 for archive or 100 km^2 tasking orders, up to a maximum of 10,000 km^2 per order. Products are delivered on the choice of standard digital media with Image Support Data files including image metadata. In this work, the specific products correspond to Standard-2A or Ortho Ready Standard-OR2A of multispectral and panchromatic data in GeoTIFF format. The corrections applied are radiometric, sensor, and geometric mapped to a cartographic projection, projected to a constant base elevation to allow for orthorectification.

ENVI 5.3 ("ENvironment for Visualizing Images") software was utilized to process and analyze the three images. Specifically, QUAC® AC method for multispectral and hyperspectral imagery was applied, working with the visible and NIR through shortwave infrared (VNIR-SWIR) wavelength range. QUAC® determines atmospheric correction parameters directly from the observed pixel spectra in a scene, without ancillary information. ENVI uses the latest QUAC algorithm described in Bernstein et al. (2012), which contains several enhancements to improve the accuracy of the AC implementation. The digital numbers (DN) recorded at the sensors were converted to satellite radiance using the metadata included from Digital Globe. QUAC creates a surface reflectance image (dimensionless), scaled into two-byte unsigned integers using a reflectance scale factor of 10.000.

2.3. Additional data

2.3.1. Real-time hopper dredger position

The vessel THOR R (IMO: 8325262, MMSI: 219573000) is a hopper dredger built in 1984 and currently sailing under the flag of Denmark. This boat was selected by the Port of Seville Authority to accomplish

the major capital dredging project started on 14 October and ended on 3 December 2016. THOR R has 80 m length overall and beam of 14 m, with a gross tonnage of 2147 tons and a deadweight of 2087 tons. In order to track the hopper dredger situation during the operations, Automatic Identification System (AIS) service was employed, specifically Terrestrial receivers, which provide near real-time updates of vessel positions from Marine Traffic (https://www.marinetraffic.com/). Thanks to this system, dredger information and positional data can be electronically exchanged between AIS stations. Data is delivered in CSV format offering longitude, latitude, vessel, status, speed, course, heading and timestamp (GMT) in addition to port calls (port ID, port name). Time resolution of data depends on a number of parameters at the specific point and time; for a moving vessel intervals may vary from a few minutes up to several hours as this case. This information was used so as to analyze it in combination with satellite data and estimate the time interval and status of the dredger at the same time that image acquisition.

2.3.2. Meteorological and oceanographic data

Daily mean discharge at the Alcalá del Río dam, the main freshwater input to the Guadalquivir estuary, was obtained from the Junta de Andalucía Regional Water Management Agency (http://www.chguadalquivir.es/saih/) at station code E60 (37.51°N–5.97°W, Fig. 1). Díez-Minguito et al. (2012) described the three hydraulic regimes of the estuary depending on river discharge from the dam: tidally dominated ($< 40\ m^3/s$), intermediate stage (40–400 m^3/s) and fluvially dominated ($> 400\ m^3/s$). Additionally, daily precipitation measured at an automatic meteorological station in Sanlúcar la Mayor (code 13, 37.42°N–6.25°W, Fig. 1) was acquired from the regional Agroclimatic Station Network (http://www.juntadeandalucia.esagriculturaypesca/ifapa/ria/servlet/FrontController). To examine tidal effects, water level data at hourly intervals was recorded by a tidal gauge property of Puertos del Estado (http://www.puertos.es/es-es) placed at the Port of Seville (37.32 °N–6.01°W, Fig. 1).

2.4. Methods

In order to estimate TSS concentration with satellite imagery during the dredging activities, a multi-conditional remote sensing algorithm recently developed with Sentinel-2A data by Caballero and Navarro (2016a) was applied. This model was adapted and regionalized in the moderately turbid coastal region of the Guadalquivir estuary and Cádiz Bay based on the methodology exposed in Novoa et al. (2017). The model has a switching method that automatically selects the most sensitive TSS vs. water reflectance relationship, thus established to estimate TSS concentration while avoiding saturation effects. The semi-analytical model of Nechad et al. (2010) was re-calibrated based on both surface reflectance (ρw) of the red (665 nm) and NIR (865 nm) parts of the spectrum. The mathematical formulation of the model is defined as (Nechad et al., 2010):

$$TSS\left(\frac{\mathrm{mg}}{\mathrm{L}}\right) = \frac{Ax\ \rho w}{1 - \frac{\rho w}{C}} + B \quad (1)$$

where: ρw corresponds to the water reflectance, C (dimensionless) is defined utilizing standard data computed from the literature (for the red and NIR bands C is equal to 0.1728 and 0.2115, respectively; Table 1 in Nechad et al., 2010), B (mg/L) represents measurement errors in both reflectance and TSS, and A (mg/L) is the calibration parameter relating reflectance to TSS. For this analysis both coefficients A and B were derived by non-linear robust weighted regression to find the best-fit values (Caballero and Navarro, 2016a).

A cross-validation procedure was carried out with in-situ TSS observations (ranging from 80 to 420 mg/L) so as to reveal the high level of robustness with respect to accuracy along the first year of Sentinel-2 data (Caballero and Navarro, 2016a). The accurate performance of the final model based on both red (r = 0.80, NRMSE = 25.06%) and NIR (r = 0.98, NRMSE = 10.28%) parts of the spectrum highlighted the MSI sensor's great potential to estimate TSS even though it was not designed for aquatic remote sensing, being applicable to the latest generation of ocean color sensors. Since the red reflectance is constantly saturated (Fig. 2) in the upstream part of the estuary close to the Port of Seville where the hopper dredger was working, the water reflectance of the NIR band (ρ_{NIR}) was selected to calculate TSS in all the imagery applying Eq. (2) (Caballero and Navarro, 2016a).

$$\mathrm{TSS\ (mg/L)} = \frac{9001 \times \rho_{NIR}}{1 - \rho w_{NIR}/0.2115} + 44 \quad (2)$$

In addition, as NIR band was used to further estimate TSS concentration, a comparison of surface reflectance between the three atmospheric procedures was accomplished in two specific areas: Area 1 (37.316°N–6.01°W) and Area 2 (37.31°N–6.019°W). These areas corresponded to two regions of interest along the estuary with a section of 30 × 30 m (900 m^2) with Landsat-8 as reference (see location in Fig. 3b). For the remaining satellites, arithmetic mean within the 30 × 30 m area was calculated in each case according to the different spatial resolutions. Currently, none of both processors Sen2Cor and QUAC have sun glint correction, whereas ACOLITE implementation corrects for low intensity of sky and glint levels. Recent studies (Caballero and Navarro, 2016a; Navarro and Caballero, 2017) show the severe sky and sun glint issues during spring and summer scenes in 2016 strongly restricted the number of MSI usable images corrected by ACOLITE procedure in the Guadalquivir estuary. On the contrary, no sun glint effects were encountered from October to December 2016 at these latitudes. In this regard, we could admit that during the dredging activities in 2016 (Table 1), minimum or nonexistence levels of glint were characterized within the estuary.

The Normalized Difference Water Index (NDWI) by McFeeters (1996) was used to create a threshold mask allowing the separation of water and land. This procedure was accomplished in ENVI for each atmospherically corrected image since the spatial resolution and the tidal range was different in each scene (Table 1). In this regard, minimum water area in the region of interest was encountered for MSI image on 4 October since the flow direction at the time of acquisition was downstream (tidal stage = −0.17 m, Fig. 3c), compared to MSI on 23 November which was characterized by an upstream flow (tidal stage = 1.44 m, Fig. 3g). This methodology has already proven its precision in previous works using the medium spatial resolution data (22 m) of Deimos-1 satellite in the Guadalquivir estuary (Caballero et al., 2014b). In order to classify and mask out the pixels within the hopper dredger and its shadow, a visual inspection of the RGB images for each scene was conducted in ENVI. In this regard, all the pixels that corresponded to both the dredger and the shadow, as well as mixed pixels (water-dredge or shadow), were removed for further analysis. Future implementations for operational services will be focused on addressing this step by means of a semi-automatic procedure. The calibrated model was then applied to all water pixels producing synoptic images of TSS and a color table was applied to the images to aid in visualization.

3. Results

3.1. Atmospheric correction performance

Qualitative inspection of the data suggested that the three available AC schemes seemed to properly correct reflectance in each satellite, with realistic spectral signatures for the six images. The commercial satellites do not have spectral bands in the SWIR, and in the NIR region, water reflectance is not zero when sediments are present in high concentration, as during dredging operations (Vanhellemont and Ruddick, 2015, 2016). In order to prove that AC effectively worked well in commercial satellites, a comparison of spectral signatures to check the

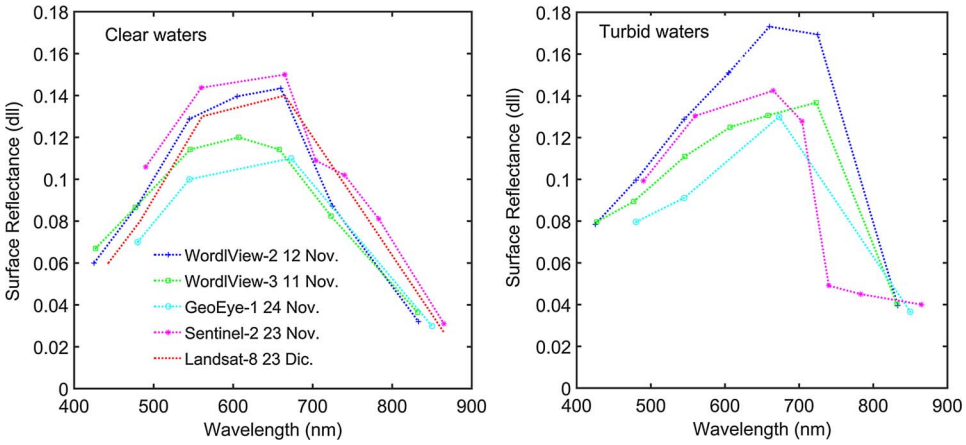

Fig. 2. Surface reflectance mean values (dimensionless, dll) averaged within a 30 × 30 m area for each of the satellites after AC. Left panel corresponds to clear waters at the entrance of the Port of Seville (6.010°N–37.317°W) and right panel corresponds to turbid waters within the turbidity plume generated by the dredging.

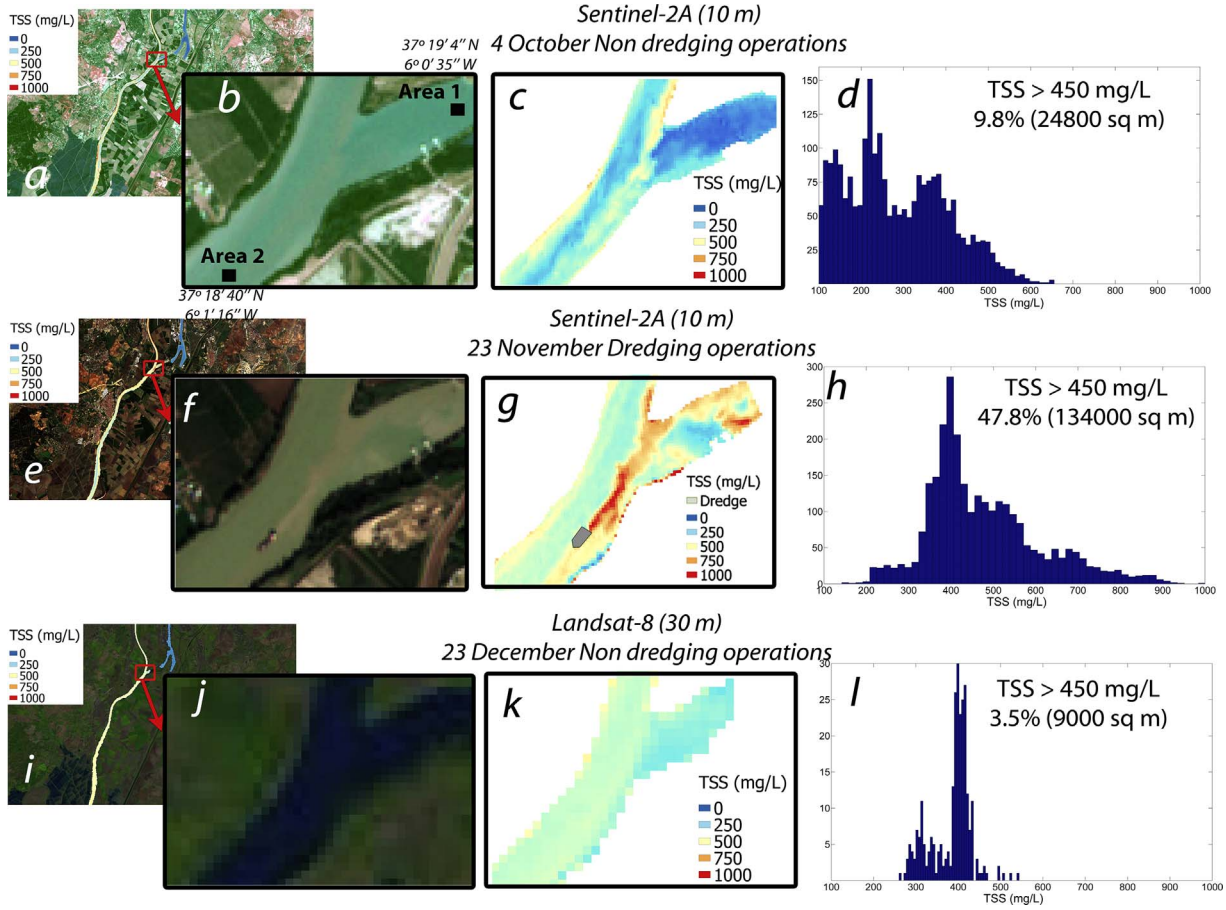

Fig. 3. a) Map showing the Guadalquivir estuary RGB composite and TSS concentration of Sentinel-2 image at 10 m spatial resolution on 4 October 2016 with red rectangle delimiting the Region Of Interest (ROI, 37°18′40″N–6°1′16″W to 37°19′4″N–6°0′35″W, Fig. 1) at the entrance of the Port of Seville, b) RGB composite, c) TSS concentration within the ROI, and d) Histogram of TSS within the ROI; e–h) the same for Sentinel-2 image on 23 November 2016. The hopper dredger and its shadow are masked at this stage in this scene; i–l) the same for Landsat-8 image at 30 m spatial resolution on 23 December 2016. Differences in TSS concentration between the main river channel (> 250 mg/L) and the parallel channel crossing the city of Seville (< 200 mg/L) are evident in the three images (a, e, i). Table 1 shows image features and oceano-meteorological conditions for each scene. (For interpretation of the references to colour in this figure legend, the reader is referred to the web version of this article.)

behavior of targets after the AC routine was accomplished. To show suitability of each methodological performance, Fig. 2 shows surface reflectance of the imagery after AC, presenting the average within a 30 × 30 m area in clear waters at the entrance of the Port of Seville (6.010°N–37.317°W) and in turbid waters within the turbidity plume generated by the dredging. Note that the reference processor is ACOLITE after the application of the SWIR AC option to correct for aerosols. The good accomplishment of the three AC schemes is observed in clear and turbid regions, with increment of surface reflectance in the turbid areas due to the augment of suspended particles scattering during dredging operations. In this regard, varying TSS levels within the turbidity plume are distinctively affecting the spectral signal of the visible and NIR bands for each dredging situation. Some of the discrepancies in clear waters may be caused, in addition to the AC models and the not identical bandwidths of each sensor, by the dynamic natural spatio-temporal variability of the optical characteristics of the water, since each image corresponds to a scene with specific tidal and oceanographic conditions. Despite the differences, the spectral shape gives us

information about the good performance of each AC model, specifically in the NIR band. Realistic spatial patterns of marine reflectance were retrieved with this recommended configuration, allowing proper evaluation of potential applications in coastal waters (Vanhellemont and Ruddick, 2015, 2016; Pahlevan et al., 2017). ACOLITE has proven to be a very accurate scheme in the processing of medium-resolution images for coastal applications (Vanhellemont and Ruddick, 2016; Novoa et al., 2017), and more specifically, in the coastal waters of the Guadalquivir estuary (Caballero and Navarro, 2016a; Navarro and Caballero, 2017). The employment of the SWIR atmospheric correction procedure with Landsat-8 image seemed to properly correct atmospheric features of the OLI bands over the Guadalquivir region, yielding reasonable spectral signature compared (Vanhellemont and Ruddick, 2015).

In addition, as NIR band is used to further estimate TSS concentration, it is presented the example of the mean NIR reflectance within two specific areas: Area 1 at 37.316°N–6.01°W and Area 2 at 37.31°N–6.019°W, both with a section of 900 m^2 (Fig. 3b). The analysis of the variability in each of the 6 scenes exhibits NIR reflectance has been accurately derived by the three AC procedures (Table 1) with the standard deviation (SD) in each area corresponding to: SD = 0.0053 (Area 1) and SD = 0.0059 (Area 2). When comparing ACOLITE with Sen2Cor and QUAC performances, similar reflectance patterns are retrieved along the spectrum (Fig. 2). Toming et al. (2016) have recently applied Sen2Cor processor for small lake mapping with precise results. In addition, validation of Sen2Cor in the turbid Albufera, Valencia coastal lagoon (Spain) and the clear oligotrophic high-altitude Lake Titicaca has also indicated good performance when compared to in-situ reflectances (Ruescas et al., 2016). In addition, QUAC has been previously examined in high-resolution commercial satellites such as QuickBird (Frasquet et al., 2012) or the hyperspectral sensor Airborne Imaging Spectrometer for Applications (AISA) (Moses et al., 2012), demonstrating robust performances for water quality studies. Ruddick et al. (2016) described the new opportunities and challenges for high-resolution remote sensing of water color by exploiting the use of these sensors in coastal and inland waters. However, in-situ and satellite radiometric match-ups would be necessary to draw further conclusions regarding the atmospheric correction implementations and their accuracy over this coastal region. In this context, it is suggested an extensive program of calibration/validation efforts over different water and atmospheric conditions in order to advance the potential of medium and high spatial resolution missions for the challenging coastal management of this environment.

3.2. Analysis of natural background and dredging-induced changes in Total Suspended Solids

3.2.1. Public satellite imagery: Landsat-8 and Sentinel-2

Fig. 3 shows the application of the algorithm (Eq. (2)) to two images of Sentinel-2A on 4 October and 23 November 2016 and one image of Landsat-8 on 23 December 2016. The dredger was working in the upstream region of the estuary at the time of acquisition of the scene on 23 November 2016. No other image of both satellites could be analyzed due to intense cloud coverage during the dredging period. Unfortunately, there were not coinciding days of Landat-8 overpasses and dredging operations during the last years of active dredging to assess if OLI at 30 m was capable of detecting these activities. Fig. 3a, e and i present TSS concentration along the estuary channel superimposed on the RGB (bands 4-3-2) composite of each image, evidencing the feasibility of TSS monitoring in the coastal and inland waters at moderately resolution (10–30 m). Differences in TSS concentration between the main river channel (> 250 mg/L) and the parallel channel crossing the city of Seville (< 200 mg/L) are evident in all the images. The figure also shows the high spatial and temporal variability of TSS typical of this estuary which is frequently influenced by intense turbidity events (Navarro et al., 2011, 2012 ; Ruiz et al., 2015). Specifically, Fig. 3c, g and k show the mapping of TSS over a zoom at the entrance of the Port of Seville within a specific ROI (37°18′40″N–6°1′16″W to 37°19′4″N–6°0′35″W, Fig. 1). The different resolution of each satellite with 10 m for Sentinel-2 and 30 m for Landsat-8 can be clearly observed in the size of the pixels. Sentinel-2 and Landsat-8 provide a significant improvement in resolution compared to previous studies carried out in this coastal fringe by mean of standard ocean color sensors such as MODIS at 1 km (Caballero et al., 2014a) and MEdium Resolution Imaging Spectrometer (MERIS) at 300 m (Caballero and Navarro, 2016b). The turbidity plume associated with the dredging operations is shown in Fig. 3g, with high TSS values and peaks of 1000 mg/L in the proximity of the dredger in contrast with waters non influenced by the operations (~ 200 mg/L). Table 1 shows the mean river discharge from Alcalá del Río dam (Fig. 1) the day of the satellite overpass and three previous days, the hydraulic regime of the estuary during this period (Díez-Minguito et al., 2012) and the tidal stage at the time of image acquisition (Fig. 1). Since the fluvial influence is minimal and the tide is flooding at the time the image in Fig. 3g was acquired (Table 1), the turbid waters generated by the dredge are moving upstream. Fig. 3d, h and l present the histograms of the ROI in each of the images. The difference between background TSS concentration, mainly influenced by discharge from Alcalá del Río dam and tidal resuspension (Navarro et al., 2011, 2012; Caballero et al., 2014a, 2014b; Ruiz et al., 2015) and dredging period mean values is used for the estimation of dredging-induced turbidity at the time of dredging operations.

The Central Dredging Association (CEDA) established that impacts of dredging-induced turbidity should be evaluated as an increase above background level, not as absolute values (CEDA, 2011). The difference between TSS maps for dredging and non-dredging periods was used here for the estimation of the increased turbidity at the time of operations, highlighting the extent and intensity of the plume impact. Fig. 3c and k shows both pre- and post-dredging situations, two examples of the natural variability of TSS along this river transect. The threshold TSS value of 450 mg/L was selected as the limit to estimate the area where turbidity is dredging-induced since the percentage of pixels above this threshold in non-dredging images is always less than 10%, as a 90th percentile. Background TSS natural variability in the upper part of the estuary retrieved from in-situ observations had not reached this limit during the tidally-dominated or the intermediate hydraulic regime (Ruiz et al., 2015). On 23 November 2016, 47.8% of pixels (134,000 m^2) are above this threshold, contrary to the low proportion of 9.8% on 4 October (24,800 m^2) or 3.5% on 23 December (9000 m^2), thus the maximum turbid area in this transect is clearly established.

3.2.2. Commercial satellite imagery: WorldView-2/-3 and GeoEye-1

Fig. 4 displays the application of the algorithm (Eq. (2)) to the very high-resolution images of WorldView-3 on 11 November (a–d), WorldView-2 on 12 November (e–h), and GeoEye-1 on 24 November 2016 (i–l), all of them capturing the hopper dredger intensively working at the entrance of the Port of Seville within the ROI (same than Fig. 3). The turbidity plume is neatly evident in the RGB composites, in the panchromatic images and in the final TSS maps, each one with less than 2 m spatial resolution. In comparison with Landsat-8 and Sentinel-2, the specific products of Ortho Ready Standard-OR2A enable accurate retrievals of water quality parameters at extremely fine scale, which is particularly useful for monitoring dredging activities along narrow channels. The RGB composites (a, e, i) and the panchromatic imagery (b, f, j) up to 0.3 m spatial resolution allow easily distinguish the vessel characteristics as well as river constructions (e.g. floodgate structures) since they are highly reflective structures. Resuspension of dredged sediments at the designated operational site is visible in each image. Natural small-scale variability in suspended sediment can also be observed, such as the streaks of sediments related to resuspension or small swirls.

TSS maps determined by the multi-conditional algorithm (c, g, k) show the formation of turbidity plumes around the hopper dredger at

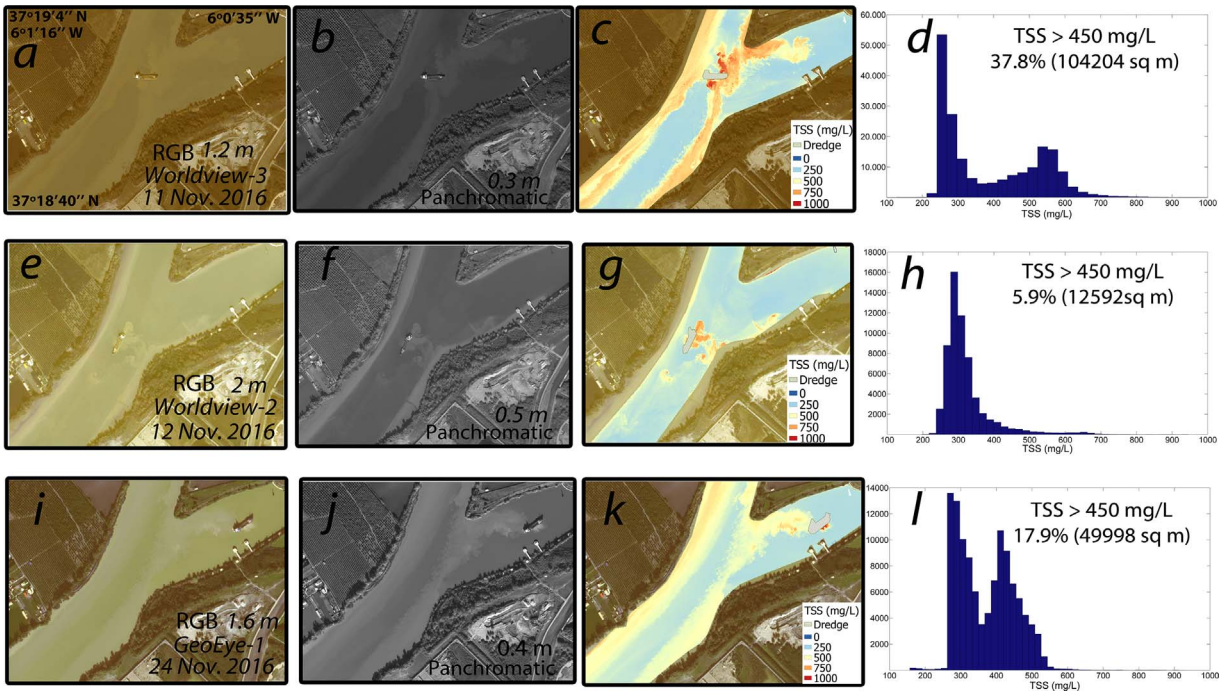

Fig. 4. a) Map showing the Guadalquivir estuary RGB composite of WorldView-3 image at 1.2 m spatial resolution on 11 November 2016 within the Region Of Interest (ROI, 37°18′40″N–6°1′16″W to 37°19′4″N–6°0′35″W, Fig. 1) at the entrance of the Port of Seville, b) Panchromatic image at 0.3 m resolution, c) TSS concentration within the ROI at 1.2 m, and d) Histogram of TSS within the ROI; e–h) same for WorldView-2 image on 12 November 2016 at 2 m spatial resolution (RGB) and 0.5 m (panchromatic); i–l) same for GeoEye-1 image on 24 November at 1.6 m spatial resolution (RGB) and 0.4 m (panchromatic). The hopper dredger and its shadow are masked at this stage in each scene. Table 1 displays image features and oceano-meteorological conditions for each scene.

each site, with TSS reaching maximum values of 900 mg/L in comparison with natural background adjacent waters (< 450 mg/L), similar to TSS values derived with Sentinel-2 on 23 November (Fig. 3g). These maps very sharply identify the regions where water quality parameters were influenced by dredging works. The areal extent and mean concentration of dredging plume can also be related with tidal conditions and the hydraulic regime (Díez-Minguito et al., 2012). The three images correspond to a tidally-dominated (WorldView-2, WorldView-3) or intermediate regime (GeoEye-1) with minimum river discharge from Alcalá del Río dam and a flooding tidal stage (Table 1). Therefore, determination of deviations from background TSS concentrations near the Port of Seville where dredging works are conducted can be effectuated. Fig. 4d, h and l display the histograms in each image detailing the variability of TSS within the ROI, with maximum extension of the plume on 11 November (37.8%, 104,204 m^2), followed by the scenes on 24 November (17.9%, 49,998 m^2) and 12 November (5.9%, 12,592 m^2). Part of the high TSS values is also related to the resuspension of the margins because of the shallower depth, as can be observed on 11 and 24 November. In regions or periods with high and moderate background TSS level, such as during intense discharges from Alcalá del Río dam (fluvially dominated regime) (Díez-Minguito et al., 2012, 2014), dredging impact might be less detectable over the natural background. Due to high cloud coverage during the study period, there was no image with these conditions to further apply the multi-conditional algorithm. For a management perspective, there is a need to know the spatial extent across the whole operational period, which makes the satellite-based method require other ancillary data such as turbidity loggers to provide valuable useful spatial data in operation management.

These results demonstrate the feasibility of commercial remote sensing to detect suspended sediments from dredging and dumping operations at fine spatial resolution (< 2 m) along narrow channels, but at the cost of very poor temporal resolution. Cloud coverage is an unexpected event, and this is not only the problem of the commercial satellites but also the publicly available ones. The early Sentinel-2A release status also evidenced that the frequent sky conditions with extensive cloud coverage and sun glint affected more than 60% Sentinel-2A images at these latitudes.

4. Discussion and conclusions

The results of this work provide evidence of the potential of public cost-effective medium spatial resolution data from Landsat-8 and Sentinel-2 for monitoring dredging plumes (Fig. 3). As both missions are close in local acquisition times, the seamless combination of Sentinel-2 data with historical images of Landsat-8 makes it possible to build long time series. Both platforms also provide true color images at 30–10 m resolution, able to resolve operations and plume features (Fig. 3b, f and j). In addition, the combined results presented in Figs. 3 and 4 confirm the viability of tracking sediment plumes along narrow channels through a combination of public and commercial medium- to high-resolution imagery. To our knowledge, this is the first time gathering of the three commercial satellites and the two public is fulfilled in order to monitor turbidity during dredging operations. This study demonstrates the detection and flagging of high TSS concentration of dredging-affected areas is feasible at fine (< 30 m) spatial scale by means of a multi-sensor approach. The methodology implemented delivers consistent outputs across the different satellite sensors restricted to where the spatial resolution of the instrument is still able to resolve the estuary width. Offshore dumping of sediments dredged from harbors in the Belgian coastal waters has been previously observed on Landsat-8 imagery by Vanhellemont and Ruddick (2014, 2015). Wu et al. (2007) examined the increase of water turbidity during the dredging works in Poyang Lake using MODIS and Landsat images. Recently, Barnes et al. (2015) studied the sediment plumes induced by the Port of Miami dredging using Landsat and MODIS data. Evaluation of Landsat data for operational monitoring of sediment plumes produced by dredging has also been carried out in Australia (Islam et al., 2007). Despite the great ability, frequent sky condition with extensive cloud coverage may limit the temporal resolution, as in this case study,

affecting more than 50% Sentinel-2A images over this region. The Copernicus Earth Observation Sentinel-2B has joined its twin satellite Sentinel-2A on 7 March 2017. With both Sentinel-2A and -2B simultaneously in operation, images will be available every five days at the Equator and more frequent at higher latitudes. This increased frequency will mean that remotely sensed data can be obtained at a temporal resolution more suitable to the monitoring demands of environmental agencies. Moreover, earlier studies revealed the potential of very high-resolution optical satellite imagery to monitor water quality of coastal and inland waters using Worldview-2 (Liew et al., 2011; Dekker and Hestir, 2012) and Quickbird (Somvanshi et al., 2011) or to map bathymetry and benthic habitat mapping of shallow-water environments with Worldview-2 (Eugenio et al., 2015).

Likewise, the three AC schemes seem to properly correct surface reflectance in the NIR, as is the band utilized to calculate TSS concentration. Eq. (2) was developed for Sentinel-2A using the NIR wavelength at 865 nm (33 nm of bandwidth). Landsat-8 has a NIR band centered at the same wavelength (28 nm of bandwidth); thus minimum uncertainties might result by applying the algorithm to OLI data. Recently, Pahlevan et al. (2017) confirmed by means of a qualitative and quantitative examination of water reflectance products that both OLI and MSI offer high consistency with in-situ observations, demonstrating very good agreement between TSS products derived from both missions in an inland system. For accurate quantitative monitoring of TSS, sensors are needed with a red (or red-edge) and NIR band, sufficiently high signal-to-noise ratio and good digitization, e.g. 10 or 12 bits (Ruddick et al., 2016). The commercial satellites, WorldView-3 and WorldView-2 have a NIR band centered at 833 nm (770–895 nm) while GeoEye-1 has it at 850 nm (780–920 nm). In this case, it is assumed to find larger uncertainties using the high-resolution NIR bands, as their bandwidths are wider compared to the medium-resolution OLI and MSI observations. Specifically, it is suggested that a certain level of overestimation in TSS concentration (Fig. 4) must be encountered in the commercial sensors, even though the accurate performance of the NIR model ($r = 0.98$, NRMSE = 10.28%). In this regard, particular emphasis must be promptly focused on dealing with additional field campaigns, including both TSS and radiometric measurements, in order to establish up-to-date information about the different spectral features and validate high-resolution satellite performances.

An adjustment of this methodology can be adopted for the assessment of many other impacts resulting from human activities in the coast, with a potential large pool of end users from national institutions interested owing to its effectiveness and cost-efficiency. This adaptation can benefit from the implementation of the novel multi-conditional algorithm to precisely estimate TSS over a wide range of concentrations such as those observed in the Guadalquivir estuary. Emerging methodologies in the published literature have been recently considered in order to overcome signal saturation and select suitable bands and algorithms to provide precise TSS retrieval from low- to high-turbidity waters. These methods focused on multi-conditional algorithm schemes composed of various TSS models, as they established to offer a more efficient and accurate estimation of TSS levels over a wide range of turbid waters and situations (Feng et al., 2014; Han et al., 2016; Novoa et al., 2017). This research based on the novel results by Novoa et al. (2017), which demonstrated accurate performance in previous coastal studies using other multispectral sensors, allow to precisely monitor TSS without the need for field radiometric measurements. However, there are components that must be taken into account when dealing with the same methodology in other environments. The calibration and validation of the algorithms to estimate water quality parameters, in this case TSS, must be accomplished with in-situ measurements in order to develop a regional or local model to further exploit the multi-sensor approach. The atmospheric correction procedures need to be tested so as to assess their performance over optically complex waters such as estuaries, lakes, rivers, and coastal areas.

The approach is currently applicable for the entire estuarine system, for real-time monitoring and for analysis of the historical data archive. The multi-sensor initiative could be then applied with confidence to efficiently guide in the decision-making processes of the works before, during and after dredging (CEDA, 2015). It can, for instance, be implemented in the design of routine operations with the aim to remove sediment as efficiently as possible while diminishing environmental impacts, most notably the re-suspension of sediments, on sensitive parts of the ecosystem. The emergence of these high-resolution satellites with new spectral channels will increase the amount of available data, thereby enhancing their applications focused on coastal management assistance. However, in this case, because of cloud coverage and the availability of very high spatial resolution images (commercial satellites capture images on demand), the best effectiveness can be achieved combining both satellite data and in-situ measurements for high temporal resolution. Nevertheless, it must be reconfirmed remote sensing techniques offer additional benefits in terms of spatial resolution compared to the conventional in-situ measurements.

The multi-sensor approach shows the great potential of these medium- to high-resolution satellites to accurately estimate TSS in highly dynamic waters (Caballero et al., 2014a, 2014b) even though they were not designed for aquatic remote sensing. These findings can immediately serve as an invitation to tender novel research based on these emerging platforms. The possibility of using a constellation of commercial optical satellites supplementing open access data to complete the temporal coverage at these coastal scales would provide researchers, policy makers and end users with novel insights and understanding of variability of these heterogeneous coastal environments. The quality of the data obtained and its high-resolution can be used for cost-efficient post-dredging monitoring, for prediction of the effects of dredging, for design and understand operational requirements, and for frequent validation and calibration of sediment transport models in combination with hydrodynamic simulations (Fettweis et al., 2007). In the case of the Guadalquivir estuary, it is a well mixed mesotidal system with a longitudinal salinity gradient (Vanney, 1970), and it is important to note that the minimum water depth is 6.5 m. Recent studies through modelling or in-situ experiments demonstrated strong mixing is typical along its extension from the Alcalá del Río dam to its mouth at Sanlúcar de Barrameda, with surface samples representative of values in most of the water column (Díez-Minguito et al., 2012, 2014; Flecha et al., 2015; Ruiz et al., 2015, 2017). The principle of estimating TSS in rivers by satellite images is based on the fact that sediment particles are well distributed, and for the case of dredging activities, estimated TSS may only represent for surface TSS due to water turbulence. Careful inspection must be further accomplished in order to account for the vertical distribution over other environments to fully address monitoring of turbidity plumes in shallow water environment.

Particularly, the satellite-based system in this study was developed in a highly sensitive environment. These findings also have projections over the local management options of the Guadalquivir estuary. The lower reaches of the estuary are adjacent to the Doñana National and Natural Park, a protected area of marshes, shallow streams, and sand dunes with a biodiversity that is unique as the largest natural reserve in Europe (Fernández and Novo, 2007). Dredging of the estuary has been extremely controversial for its impact on this preserved area as well as on the nursery role of the estuary mouth where recruitment of important fishery species occurred (González-Ortegón et al., 2010; Ruiz et al., 2015). Owing, among others, of these potential repercussions, the dredging activities conducted by the Port Authority of Seville are frequently under social scrutiny and controversy. Furthermore, past decisions by the Port Authority of Seville to extend the program of dredging so as to significantly increase the depth and width of the navigational section has triggered even more alarm. This possibility will accumulate to the historical impacts the estuary has already received (Ruiz et al., 2017). The strategy presented here can be used to advance the management of the estuary and its surrounding areas in order to diagnose and prognose the possible consequences of this type of action

on the ecosystem, where increased bathymetry might lead to increased currents and turbidity levels. Thus, this study highlights the great benefit for a cost-effective operational service of determining sediment plume dynamics and its influence on the fringing environment for management purposes, as well as the ability to communicate to society the impact of dredging activities on both the estuary and its area of influence. In addition, continuous monitoring through signature-based imagery techniques can provide for the first time high-resolution data regarding sedimentation, which can be significantly helpful for the coastal area designers, stakeholders and decision-makers.

Dredging activities can have great environmental repercussions and in recent years, awareness of these impacts has grown, on the client side as well as among contractors (CEDA, 2011). Specifically, dredge and fill activities in estuaries have many ecological effects, most of them deleterious, such as the reduction of light penetration by increased turbidity and release of contaminant in the water column (Johnston, 1981; Vargas and Paneque, 2015; Ruiz et al., 2015, 2017). The main potential impacts on flora from dredging and sand mining include physical removal and burial of vegetation and effects of increased turbidity and sedimentation (Erftemeijer and Lewis, 2006). Therefore, ways to mitigate the effects of dredge and fill operations include careful pre- and post-operation environmental studies (Johnston, 1981; CEDA, 2011). The large-scale dredging programs typically involve several types of monitoring, both surveillance or baseline and feedback or adaptive monitoring, the first acts as a reference for the interpretation of dredging impacts and the second for the verification of pre-project environmental assessments (model predictions, expert judgment), providing a base for possible adaptation of the project design, planning and/or work method (CEDA, 2011). Our findings are promising for future environmental monitoring owing to the increased capacity of new sensors to provide fine-scale spatial maps of water quality in nearshore and estuarine areas. This is the key strength of the study, and it is essential that these results are coupled with fine temporal scale monitoring at sentinel locations, due to the temporal coverage archived using satellite-based schemes is not sufficient for compliance monitoring. Furthermore, the noticeable advantage of emerging geostationary sensors will offer the basis for future superior temporal resolution of TSS maps, providing several images per day compared to once per day of standard multiespectral satellites. Neukermans et al. (2012) already demonstrated, using the Spinning Enhanced Visible and Infrared Imager (SEVIRI) geostationary platform with availability of images every 15 min, the possibilities of these improved applications including the examination of high frequency dynamics of the coastal ecosystem. This new flow of information should benefit the assessment and monitoring abilities of environmental agencies, reduced costs and encourage stakeholder involvement as well as enhance public awareness.

Additional research must be focused on the continuity of the Copernicus services relying on multi-spectral high spatio-temporal resolution observations in order to establish an advanced framework along coastal and inland waters, with an increasing demand for guidelines and recommendations by the research community and particularly, for end users and water managers. However, even if additional insights might be tested for a multi-mission applicability over a wide range of TSS concentrations, this approach provided a precise portrait enhancing the consistent quantitative estimation of sediment concentration as a reference dataset with semi-automated methods. In addition, the study highlighted the novel MSI sensor's great potential to estimate TSS even though it was not designed for aquatic remote sensing, being applicable to the latest generation of ocean color, land-based or commercial sensors. Therefore, these emerging technologies will substantially support operational and policy needs for the challenging marine management as key contributions to the Earth Observing Program.

Acknowledgments

The authors would like to thank the ESA and the Copernicus Program for distributing the Sentinel-2 data used in this study and the USGS and NASA for Landast-8 data. Thanks to Quinten Vanhellemont at the Royal Belgian Institute for Natural Sciences (RBINS) for his assistance in using ACOLITE processor. In addition, the authors thank the anonymous reviewers for their suggestions that have significantly improved the manuscript.

Isabel Caballero is supported by a postdoctoral grant from the Junta de Andalucía fellowship program. The commercial imagery from WordlView-2/-3 and GeoEye-1 are provided by the European Space Agency in the framework of a Third Party Mission Project (id35116). This work was partially supported by the Projects P09-RNM-4853, PR11-RNM-7722, PIE201530I012 and CTM2014-58181-R.

References

Barnes, B.B., Hu, C., Kovach, C., Silverstein, R.N., 2015. Sediment plumes induced by the Port of Miami dredging: analysis and interpretation using Landsat and MODIS data. Remote Sens. Environ. 170, 328–339. http://dx.doi.org/10.1016/j.rse.2015.09.023.

Bernstein, L.S., Jin, X., Gregor, B., Adler-Golden, S., 2012. Quick atmospheric correction code: algorithm description and recent upgrades. Opt. Eng. 51 (11). http://dx.doi.org/10.1117/1.OE.51.11.111719. 111719/1–111719/11.

CEDA Information Paper, June, 2011, (http://www.dredging.org).

CEDA Information Papers, Marchand April, 2015, (http://www.dredging.org).

Caballero, I., Navarro, G., 2016a. Sentinel-2 early efforts to support coastal management in Spain. In: Colour and Light in the Ocean from Earth Observation (CLEO). 6–8 September 2016, ESA-ESRIN, Frascati Rome (Italy).

Caballero, I., Navarro, G., 2016b. Dynamics of the turbidity plume in the Guadalquivir estuary coastal region: observations from in situ to remote sensing data. In: ESA Living Planet Symposium. 9–13 May 2016 Prage (Czech Republic).

Caballero, I., Morris, E.P., Prieto, L., Navarro, G., 2014a. The influence of the Guadalquivir River on spatio-temporal variability in the pelagic ecosystem of the eastern Gulf of Cádiz. Mediterr. Mar. Sci. 15 (4), 721–738. http://dx.doi.org/10.12681/mms844.

Caballero, I., Morris, E.P., Ruiz, J., Navarro, G., 2014b. Assessment of suspended solids in the Guadalquivir estuary using new DEIMOS-1 medium spatial resolution imagery. Remote Sens. Environ. 146, 148–158. http://dx.doi.org/10.1016/j.rse.2013.08.047.

Díez-Minguito, M., Baquerizo, A., Ortega-Sánchez, M., Navarro, G., Losada, M., 2012. Tide transformation in the Guadalquivir estuary (SW Spain) and process-based zonation. J. Geophys. Res.: Oceans 117 (C3), 1978–2012. http://dx.doi.org/10.1029/2011JC007344.

Díez-Minguito, M., Baquerizo, A., de Swart, H.E., Losada, M.A., 2014. Structure of the turbidity field in the Guadalquivir estuary: analysis of observations and a box model approach. J. Geophys. Res.: Oceans 119 (10), 7190–7204. http://dx.doi.org/10.1002/2014JC010210.

Dekker, A.G., Hestir, E.L., 2012. Evaluating the Feasibility of Systematic Inland Water Quality Monitoring with Satellite Remote Sensing. Commonwealth Scientific and Industrial Research Organization, Canberra, Australia.

Donázar-Aramendía, I., Sanchez-Moyano, J., García-Asencio, I., Miró, J.M., Megina, C., García-Gómez, J.C., 2016. Impacts of dredged-material disposal on the soft-bottom communities in a marine dumping area near to Guadalquivir estuary, Spain. Frontiers of Marine Science Conference Abstract: XIX Iberian Symposium on Marine Biology Studies.

Dorji, P., Fearns, P., 2017. Impact of the spatial resolution of satellite remote sensing sensors in the quantification of total suspended sediment concentration: a case study in turbid waters of Northern Western Australia. PLoS One 12 (4), e0175042. http://dx.doi.org/10.1371/journal.pone.0175042.

Erftemeijer, P.L., Lewis, R.R.R., 2006. Environmental impacts of dredging on seagrasses: a review. Mar. Pollut. Bull. 52 (12), 1553–1572. http://dx.doi.org/10.1016/j.marpolbul.2006.09.006.

Eugenio, F., Marcello, J., Martin, J., 2015. High-resolution maps of bathymetry and benthic habitats in shallow-water environments using multispectral remote sensing imagery. IEEE Trans. Geosci. Remote Sens. 53 (7), 3539–3549. http://dx.doi.org/10.1109/TGRS.2014.2377300.

European Space Agency, 2015. Sentinel-2 User Handbook. ESA Standard Document, ESA, Paris, France.

Evans, Richard D., Murray, Kathy L., Field, Stuart N., Moore, James AY, Shedrawi, George, Huntley, Barton G., Fearns, Peter, Broomhall, Mark, McKinna, Lachlan I.W., Marrable, Daniel, 2012. Digitise this! A quick and easy remote sensing method to monitor the daily extent of dredge plumes. PLoS One 7 (12), e51668.

Fearns, P., Broomhall, M., Dorji, P., 2017. Optical Remote Sensing for Dredge Plume Monitoring: A Review, Report of Theme 3. WAMSI Dredging Science Node (October 2017).

Feng, L., Hu, C., Chen, X., Song, Q., 2014. Influence of the Three Gorges Dam on total suspended matters in the Yangtze Estuary and its adjacent coastal waters: observations from MODIS. Remote Sens. Environ. 140, 779–788. http://dx.doi.org/10.1016/j.rse.2013.10.002.

Fernández, J.B.G., Novo, F.G., 2007. High-intensity versus low-intensity restoration

alternatives of a tidal marsh in Guadalquivir estuary, SW, Spain. Ecol. Eng. 30 (2), 112–121. http://dx.doi.org/10.1016/j.ecoleng.2006.11.005.
Fettweis, M., Nechad, B., Van den Eynde, D., 2007. An estimate of the suspended particulate matter (SPM) transport in the southern North Sea using SeaWiFS images, in-situ measurements and numerical model results. Cont. Shelf Res. 27, 1568–1583. http://dx.doi.org/10.1016/j.csr.2007.01.017.
Flecha, S., Huertas, I.E., Navarro, G., Morris, E.P., Ruiz, J., 2015. Air-Water CO2 fluxes in a highly heterotrophic estuary. Estuar. Coasts 38 (6), 2295–2309. http://dx.doi.org/10.1007/s12237-014-9923-1.
Frasquet, M.T.S., Cremades, J.E., Alamá, M.R., Gavila, J.M., Giaccaglia, S.L.F., 2012. Estimation of chlorophyll áA« on the Mediterranean coast using a QuickBird image. Rev. Teledetec. 37, 23–33 (Asociación Española de Teledetección).
González-Ortegón, E., Subida, M.D., Cuesta, J.A., Arias, A.M., Fernández-Delgado, C., Drake, P., 2010. The impact of extreme turbidity events on the nursery function of a temperate European estuary with regulated freshwater inflow, Estuarine. Coast. Shelf Sci. 87 (2), 311–324. http://dx.doi.org/10.1016/j.ecss.2010.01.013.
Han, B., Loisel, H., Vantrepotte, V., Mériaux, X., Bryère, P., Ouillon, S., Dessailly, D., Xing, Q., Zhu, J., 2016. Development of a semi-analytical algorithm for the retrieval of suspended particulate matter from remote sensing over clear to very turbid waters. Remote Sens. 8, 211. http://dx.doi.org/10.3390/rs8030211.
Hucke, D., Hillebrand, G., Winterscheid, A., Kranz, S., Basche, B., 2016. Operational monitoring of turbidity in rivers: how satellites can contribute. Remote Sensing for Agriculture, Ecosystems, and Hydrology XVIII, 9998, 999817. International Society for Optics and Photonicshttp://dx.doi.org/10.1117/12.2241068.
IOCCG Report 10, 2010, Atmospheric Correction for Remotely-Sensed Ocean-Colour Products, Edited by Menghua Wang, pp. 78.
IOCCG Report 13, 2012, Mission Requirements for Future Ocean-Colour Sensors, Edited by Charles R. McClain and Gerhard Meister, pp. 106.
Islam, A., Wang, L., Smith, C., Reddy, S., Lewis, A., Smith, A., 2007. Evaluation of satellite remote sensing for operational monitoring of sediment plumes produced by dredging at Hay Point, Queensland, Australia. J. Appl. Remote Sens. 1 (1), 011506. http://dx.doi.org/10.1117/1.2834768.
Jørgensen, P.V., Edelvang, K., 2000. CASI data utilized for mapping suspended matter concentrations in sediment plumes and verification of 2-D hydrodynamic modelling. Int. J. Remote Sens. 21 (11), 2247–2258. http://dx.doi.org/10.1080/01431160050029549.
Johnston, S.A., 1981. Estuarine dredge and fill activities: a review of impacts. Environ. Manag. 5 (5), 427–440. http://dx.doi.org/10.1007/BF01866820.
Knight, E.J., Kvaran, G., 2014. Landsat-8 operational land imager design, characterization and performance. Remote Sens. 6 (11), 10286–10305. http://dx.doi.org/10.3390/rs61110286.
Liew, S.C., Saengtuksin, B., Kwoh, L.K., 2011. Mapping water quality of coastal and inland waters using high resolution WorldView-2 satellite imagery. Proceedings 34th International Symposium on Remote Sensing of Environment 10–15.
Müller-Wilm, U., 2016. Sentinel-2 MSI – Level-2A Prototype Processor Installation and User Manual, S2PAD-VEGA-SUM-0001, ESRIN, Issue 2.2. Telespazio VEGA Deutschland GmbH, Darmstadt, Germany.
Malenovský, Z., Rott, H., Cihlar, J., Schaepman, M.E., García-Santos, G., Fernandes, R., Berger, M., 2012. Sentinels for science: potential of sentinel-1, -2, and-3 missions for scientific observations of ocean, cryosphere, and land. Remote Sens. Environ. 120, 91–101. http://dx.doi.org/10.1016/j.rse.2011.09.026.
McFeeters, S.K., 1996. The use of the Normalized Difference Water Index (NDWI) in the delineation of open water features. Int. J. Remote Sens. 17 (7), 1425–1432. http://dx.doi.org/10.1080/01431169608948714.
Moses, W.J., Gitelson, A.A., Perk, R.L., Gurlin, D., Rundquist, D.C., Leavitt, B.C., Brakhage, P., 2012. Estimation of chlorophyll-a concentration in turbid productive waters using airborne hyperspectral data. Water Res. 46 (4), 993–1004. http://dx.doi.org/10.1016/j.watres.2011.11.068.
Navarro, G., Caballero, I., 2017. Potential of high spatial Sentinel-2A imagery to retrieve suspended solids in turbid waters. In: Satellite Validation International Workshop, Validating Copernicus Sentinel Data Using Fiducial Reference Measurements. 20–21 June Plymouth.
Navarro, G., Gutiérrez, F.J., Díez-Minguito, M., Losada, M.A., Ruiz, J., 2011. Temporal and spatial variability in the Guadalquivir estuary: a challenge for real-time telemetry. Ocean Dyn. 61 (6), 753–765. http://dx.doi.org/10.1007/s10236-011-0379-6.
Navarro, G., Huertas, I.E., Costas, E., Flecha, S., Díez-Minguito, M., Caballero, I., Ruiz, J., 2012. Use of a real-time remote monitoring network (RTRM) to characterize the Guadalquivir estuary (Spain). Sensors 12 (2), 1398–1421. http://dx.doi.org/10.3390/s120201398.
Nechad, B., Ruddick, K.G., Park, Y., 2010. Calibration and validation of a generic multisensor algorithm for mapping of total suspended matter in turbid waters. Remote Sens. Environ. 114 (4), 854–866. http://dx.doi.org/10.1016/j.rse.2009.11.022.
Neukermans, G., Ruddick, K.G., Greenwood, N., 2012. Diurnal variability of turbidity and light attenuation in the southern North Sea from the SEVIRI geostationary sensor. Remote Sens. Environ. 124, 564–580.
Newell, R.C., Seiderer, L.J., Hitchcock, D.R., 1998. The impact of dredging works in coastal waters: a review of the sensitivity to disturbance and subsequent recovery of biological resources on the sea bed. In: In: Ansell, A.D., Gibson, R.N., Barnes, Margaret (Eds.), Oceanography and Marine Biology: An Annual Review 36. UCL Press, pp. 127–178.
Novoa, S., Doxaran, D., Ody, A., Vanhellemont, Q., Lafon, V., Lubac, B., Gernez, P., 2017. Atmospheric corrections and multi-conditional algorithm for multi-sensor remote sensing of suspended particulate matter in low-to-high turbidity levels coastal waters. Remote Sens. 9 (1), 61. http://dx.doi.org/10.3390/rs9010061.
Pahlevan, N., Sarkar, S., Franz, B.A., Balasubramanian, S.V., He, J., 2017. Sentinel-2 MultiSpectral Instrument (MSI) data processing for aquatic science applications: demonstrations and validations. Remote Sens. Environ. 201, 47–56. http://dx.doi.org/10.1016/j.rse.2017.08.033.
Richter, R., Louis, J., Berthelot, B., 2011, Algorithm Sentinel-2 MSI – Level 2A Products Algorithm Theoretical Basis Document, S2PAD-ATBD-0001, Issue 2.0.
Ruddick, K., Vanhellemont, Q., Dogliotti, A., Nechad, B., Pringle, N., Van der Zande, D., 2016. New opportunities and challenges for high resolution remote sensing of water colour. In: Ocean Optics Conference. 7th October 2016.
Ruescas, A., Pereira-Sandoval, M., Tenjo, C., Ruiz-Verdú, A., Steinmetz, F., De Keukelaere, L., 2016. Sentinel-2 atmospheric correction inter-comparison over two lakes in Spain and Peru-Bolivia. In: Colour and Light in the Ocean from Earth Observation (CLEO). 6–8 September 2016, ESA-ESRIN, Frascati, Rome (Italy).
Ruiz, J., Polo, M.J., Díez-Minguito, M., Navarro, G., Morris, E.P., Huertas, E., Caballero, I., Contreras, E., Losada, M.A., 2015. The guadalquivir estuary: a hot spot for environmental and human conflicts, environmental management and governance. Adv. Coast. Mar. Resour., Springer International Publishing Switzerland 8, 199–232. http://dx.doi.org/10.1007/978-3-319-06305-8_8.
Ruiz, J., Macías, D., Navarro, G., 2017. Natural forcings on a transformed territory overshoot thresholds of primary productivity in the Guadalquivir estuary. Cont. Shelf Res. 148, 199–207. http://dx.doi.org/10.1016/j.csr.2017.09.002.
Seo, J.Y., Ha, H.K., Im, J., Hwang, J.H., Choi, S.M., Won, N.I., Kim, Y., 2018. Impact of seasonal vertical stratification on the dispersion patterns of dredging plumes off the south coast of Korea. Mar. Geol. 395, 14–21. http://dx.doi.org/10.1016/j.margeo.2017.09.005.
Sipelgas, L., Raudsepp, U., Kõuts, T., 2006. Operational monitoring of suspended matter distribution using MODIS images and numerical modelling. Adv. Space Res. 38 (10), 2182–2188. http://dx.doi.org/10.1016/j.asr.2006.03.011.
Somvanshi, S., Kunwar, P., Singh, N.B., Kachhwaha, T.S., 2011. In: Water Turbidity Assessment in Part of Gomti River Using High Resolution Google Earth's Quickbird Satellite Data. Geospatial World Forum. pp. 18–21.
Toming, K., Kutser, T., Laas, A., Sepp, M., Paavel, B., Nõges, T., 2016. First experiences in mapping lake water quality parameters with Sentinel-2 MSI imagery. Remote Sens. 8 (8), 640. http://dx.doi.org/10.3390/rs8080640.
Vanhellemont, Q., Ruddick, K., 2014. Turbid wakes associated with offshore wind turbines observed with Landsat 8. Remote Sens. Environ. 145, 105–115. http://dx.doi.org/10.1016/j.rse.2014.01.009.
Vanhellemont, Q., Ruddick, K., 2015. Advantages of high quality SWIR bands for ocean colour processing: examples from Landsat-8. Remote Sens. Environ. 161, 89–106. http://dx.doi.org/10.1016/j.rse.2015.02.007.
Vanhellemont, Q., Ruddick, K., 2016. ACOLITE for sentinel-2: aquatic applications of MSI imagery. In: ESA Special Publication, ESA Living Planet Symposium. Prague, Czech Republic. pp. 9–13.
Vanney, J.R., 1970. L'Hydrologie du bass Guadalquivir. C.S.I.C, Madrid.
Vargas, J., Paneque, P., 2015. Major hydraulic projects, coalitions and conflict. Seville's harbour and the dredging of the guadalquivir (Spain). Water 7 (12), 6736–6749. http://dx.doi.org/10.3390/w7126658.
Wu, G., De Leeuw, J., Skidmore, A.K., Prins, H.H.T., Liu, Y., 2007. Concurrent monitoring of vessels and water turbidity enhances the strength of evidence in remotely sensed dredging impact assessment. Water Res. 41, 3271–3280. http://dx.doi.org/10.1016/j.watres.2007.05.018.